JOC*Article*

Determination of the Preferred Conformation of the Bicyclic Galerucella Pheromone Using Density Functional Theory Optimization and Calculations of Chemical Shifts

Wayne B. Bosma,[†] Robert J. Bartelt,[‡] and Frank A. Momany*[,§]

*Department of Chemistry and Biochemistry, Bradley University, Peoria, Illinois 61625, Crop Bioprotection Research Unit, USDA, ARS, MWA, National Center for Agricultural Utilization Research, 1815 North University Street, Peoria, Illinois 61604, and Plant Polymer Research Unit, **USDA, ARS, MWA, National Center for Agricultural Utilization Research, 1815 North University Street, Peoria, Illinois 61604*

momanyfa@ncaur.usda.gov

Received November 30, 2005

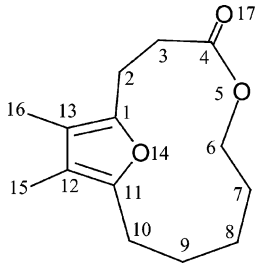

A pheromone from the beetle, *Galerucella calmariensis*, was recently isolated and identified (Bartelt, R. J. et al. *J. Chem. Ecol.* **2006**, *32*, 693−712) as a 14-carbon, bicyclic dimethylfuran lactone, with the systematic name 12,13-dimethyl-5,14-dioxabicyclo[9.2.1]tetradeca-1(13),11-dien-4-one. The main 12-membered lactone ring is very flexible; as a result, there exist multiple possible conformations. The preferred conformation cannot be deduced solely from room-temperature NMR measurements. Using density functional (DFT) studies, 26 unique conformers with energies within 10.0 kcal/mol of the global minimum-energy structure were found. A mirror-image plane exists so that each conformer has an "inverse" structure with the same energy, for which the dihedral angles around the flexible ring have opposite sign. The isotropic ^{1}H and ^{13}C NMR chemical shifts of the DFT-optimized structures were calculated using the gauge-including atomic orbital (GIAO) method. By considering the relative energies of the conformers and the calculated and observed NMR spectra, we concluded that the molecule exists primarily as a mixture of two distinct conformers at room temperature, each being present with its mirror-image inverse. Structural interconversions among these likely occur on a time scale that is fast compared to the NMR experiments. Using mode-following and dihedral-driving techniques, several potential pathways were found for the conversion of the lowest-energy conformer to its mirror-image structure. Ab initio molecular dynamics (AIMD) using the 4-31G basis set was carried out for 50 ps to test the availability of various low-energy minima and the transition states found from the searches noted above.

Introduction

The determination of the conformational ensemble of small flexible cyclic molecules in solution remains a remarkably difficult problem. First, there is the difficulty of rapid molecular movement, which defeats solution X-ray diffraction or other optical methods. Second, the conformational flexibility can cause difficulty unless an averaging method exists to allow for a population analysis. If crystallization of the molecule is possible, X-ray diffraction analysis remains the best source of structural information. However, in cases of very flexible molecules, the solid-state structure may not be the same as the preferred structure in solution. To deduce the solution-phase conformation

[†] Department of Chemistry and Biochemistry, Bradley University.
[‡] Crop Bioprotection Research Unit, USDA, ARS, MWA.
[§] Plant Polymer Research Unit, USDA, ARS, MWA.

10.1021/jo0524730 CCC: $33.50
Published on Web 05/20/2006

of a molecule, one can carefully measure the NMR spectrum and analyze the resulting chemical shifts and coupling constants. Unfortunately, when the solution phase consists of a mixture of conformers, the interpretation of the NMR data becomes less straightforward. In such cases, molecular modeling becomes an important tool in determining the likely solution-phase molecular structure.

NMR chemical shifts may be computed for chemical structures determined by ab initio techniques using the gauge-including atomic orbital (GIAO)[2] method; this procedure allows the calculation of reliable nuclear shielding tensors. Pulay et al.[3] made the suggestion that because the chemical shift range of ^{1}H is the smallest of all atoms it should be sensitive to variations in geometry, i.e., conformation. In the work reported here, a large ab initio basis set is utilized (6-311++G**) in combination with the B3LYP density functional to determine the energetically favorable conformers and NMR chemical shifts of a bicyclic dimethylfuran lactone, denoted herein as the galerucella molecule. This combination of a basis set and the density functional has been shown[4] to give very consistent and reliable structures upon geometry optimization, and these structures in turn lead to reliable chemical shifts for a series of small test molecules.[5] The use of density functional theory (DFT) is advantageous over Hartree−Fock methods because nuclear shielding constants are very correlation dependent; accordingly, the use of DFT results in a dramatic improvement in chemical shifts over traditional Hartree−Fock SCF calculations.[6,7] B3LYP was chosen because it has been shown to predict good magnetic shielding tensors for a variety of compounds containing ^{13}C, ^{15}N, ^{17}O, and ^{1}H.[7]

The particular molecule under study is the male-produced aggregation pheromone from the beetle, *Galerucella calmariensis* L. (order Coleoptera, family Chrysomelidae). Both sexes are attracted to the pheromone. This species was imported for the biological control of purple loosestrife, *Lythrum salicaria*, a nonnative plant that has become an ecologically damaging, invasive weed in wetland areas in the United States. The characterization and synthesis of this aggregation pheromone will allow for development of a sensitive monitoring tool for these beetles, to provide information on population densities, seasonal timing, dispersal rates, and other biological parameters important to land managers. The pheromone was isolated from airborne emissions from male beetles and was characterized using NMR spectroscopy, mass spectrometry, and other analytical methods as a dimethylfuran lactone[1] with the systematic name 12,13-dimethyl-5,14-dioxabicyclo[9.2.1]tetradeca-1(13)-11-dien-4-one (see Figure 1).

The lactone ring consists of 12 atoms, giving a huge number of possible conformers at any instant in time. The structures of the most stable conformers are not intuitively obvious. Although NMR spectra and the Karplus equation[8] can provide information about structural conformations, the information will be obscured

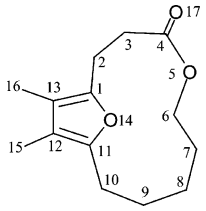

FIGURE 1. Schematic diagram of the galerucella pheromone.

if more than one conformation is present and interconversion is occurring. Even in the most favorable situations, the structures inferred from the observed NMR spectrum are not likely to be as precisely defined as those using quantum mechanical methods. Accordingly, DFT calculations were carried out to determine possible ring conformations, carefully searching for low-energy structures and comparing calculated proton and carbon chemical shifts to those obtained experimentally.

For a given molecular conformer at 0 K, the methylene hydrogen atoms on a given carbon atom will give rise to different shifts in the calculated NMR spectrum. Because the experimental ^{1}H NMR spectrum shows a single shift for each methylene group,[1] some structural averaging is occurring on a fast time scale compared to that of the NMR experiment so that both hydrogen atoms in a given methylene group see the same magnetic environment. Depending on the overall flexibility of the system and the barriers between conformers, this averaging could be due to either the fluctuations in molecular structure of a given conformer at room temperature or an interconversion between conformers on a time scale that is rapid compared to the time scale of the NMR experiment. The structural fluctuations within a single conformer will only give rise to averaged ^{1}H NMR peaks if the changes in the magnetic environment experienced by the two methylene hydrogen atoms during those fluctuations are large compared to the anisotropy between the methylene hydrogen atoms in the minimized structure. Otherwise, structural interconversion must be taking place if each methylene group gives rise to a single NMR signal.

The symmetry of the galerucella molecule is such that, for each conformer obtained, there is a mirror-image structure, obtained by reflecting the molecule through the plane of the furan ring. This inverse structure has the same energy, and all of the large ring dihedral angles have the same magnitude but opposite sign. The mirror-image structure corresponding to a given conformer gives rise to identical NMR spectra, with the ^{1}H chemical shifts exchanged for each pair of methylene hydrogen atoms in the proton NMR spectrum. Accordingly, if the potential energy landscape for this molecule is such that conformers may freely interconvert with their mirror images, the calculated chemical shifts for sets of methylene hydrogen atoms may simply be averaged.

The 1D and 2D NMR experiments provided key information about the connectivity of the atoms in the molecule, but they gave only time-averaged information about the conformation of the flexible ring. In the proton spectrum, the signals for the seven methylene groups and the two methyl groups are all distinct and separate from each other,[1] and therefore, it was immediately clear that the two protons of each methylene group have identical shifts. The splitting patterns for the methylenes at positions 2, 3, 6, and 10 have second-order character and

(1) Bartelt, R. J.; Cosse, A. A.; Zilkowski, B. W.; Weisleder, D.; Grode, S. H.; Wiedenmann, R. N. L.; Post, S. L. *J. Chem. Ecol.* **2006**, *32*, 693−712.
(2) Ditchfield, R. *Mol. Phys.* **1974**, *27*, 789−807.
(3) Wolinski, K.; Hinton, J. F.; Pulay, P. *J. Am. Chem. Soc.* **1990**, *112*, 8251−8260.
(4) Wiberg, K. B. *J. Comput. Chem.* **2004**, *25*, 1342−1346.
(5) Wiberg, K. B. *J. Comput. Chem.* **1999**, *20*, 1299−1303.
(6) Cheeseman, J. R.; Trucks, G. W.; Keith, T. A.; Frisch, M. J. *J. Chem. Phys.* **1996**, *104*, 5497−5509.
(7) Rauhut, G.; Puyear, S.; Wolinski, K.; Pulay, P. *J. Phys. Chem.* **1996**, *100*, 6310−6316.
(8) Karplus, M. *J. Chem. Phys.* **1959**, *30*, 11−15.

appear as couplets of classical aa′bb′ systems. (The signals for methylenes at positions 7, 8, and 9 are more complicated, each signal being influenced by two neighboring methylene groups rather than just one, but are still relatively simple in appearance.) The aa′bb′ appearance implies that, for adjacent methylenes, there are effectively just two vicinal coupling constants: one for protons on the same side of the ring and the other for protons on the opposite side of the ring. This simplicity argues that the molecule is not "trapped" in one conformation (where one would expect the protons of each methylene group to have different shifts and very complex splitting patterns due to a wide range of dihedral angles[8]) but, instead, that several different conformations are rapidly interconverting on the NMR time scale. The most likely explanation for the simplicity of the ^{1}H NMR spectrum is that the lowest-energy conformer (or conformers) is interconverting freely with its mirror image so that the experimentally observed chemical shifts correspond to the calculated shifts with the signals averaged for equivalent protons. To help clarify the origins of this coalescence of ^{1}H NMR peaks, room- and high-temperature ab initio (HF/4-31G) molecular dynamics (AIMD) and (B3LYP/6-311++G**) transition-state calculations were performed on the galerucella molecule. Potential interconversion pathways are described.

Methods

All energies and structures reported here were calculated using Parallel Quantum Solutions (PQS)[9] software, at the B3LYP/6-311++G** level of theory or, in the case of the dynamics simulations, at the HF/4-31G level of theory. Initial guesses for the geometries of the first few conformers that were calculated were generated using the InsightII/Discover software of the Accelrys Corporation.[10] Using the AMBER[11] empirical force field, low-energy structures were generated using dihedral constraints and energy optimization. Molecular dynamics simulations were also carried out using this empirical force field to find new low-energy conformations.

In addition to the use of the empirical force field, new local minimum-energy conformers were generated from other DFT-optimized minima by two different methods using the PQS software. The first was the use of a Hessian mode-following technique to find transition states.[12] Some 10−15 different vibrational modes were followed for a given local minimum structure to locate a transition state. From the transition states, minimization was carried out using the Intrinsic Reaction Coordinate method.[13,14] In many cases, minimization from the transition states obtained by this method resulted in new low-energy conformers. Because some initial calculations produced transition states involving only rotation of the methyl groups attached to the furan ring, most of the transition-state calculations were made on an analogue of the galerucella molecule, in which the methyl groups on the furan ring have been replaced by hydrogen atoms. Transition states (and subsequent local minima) were initially found using the HF/4-31G level of theory, and then the structures were refined using B3LYP/6-311++G**; this was done to find the energy-minimized structures more efficiently. A frequency calculation was performed for each transition-state structure, to confirm the presence of a single negative eigenvalue (i.e., imaginary frequency). It was found that following the higher-energy vibrational modes (n > 10) seldom converged to a transition state in the 200 optimization cycles allotted. Although there were noticeable differences in the optimized geometry between the two levels of theory, HF/4-31G produced structures that were sufficiently close to the DFT structures that definite identification of the minima and transition states could consistently be made.

In addition to the mode-following technique, the molecule was converted from one local minimum into another by driving individual dihedral angles in 10 degree increments through rotation about a bond of interest, with optimization of the rest of the molecule at each step. This procedure led to several of the local minima reported and gave approximate energies and geometries for several transition states. As with the mode-following technique, these calculations were performed at the HF/4-31G level of theory, followed by geometry optimization of the minima and transition states using B3LYP/6-311++G**. Some researchers have pointed out that the dihedral-driving technique does not always result in a realistic reaction path;[16] however, in the present study, the structures obtained from the dihedral-driving technique were always used as starting points for full (unconstrained) optimization. Because of the size of the large flexible ring and the large number of conformations that were obtained, neither the mode-following technique nor the dihedral-driving technique could be performed to an extent that exhausted all of the possible starting and ending points; instead, the computational effort was focused on obtaining low-energy local minima and saddle point structures that lie in the path of the inversion of the lowest-energy conformer. In the final B3LYP/6-311++G** optimization procedure, the conformers were first optimized at a smaller basis set (6-31+G*) with the B3LYP density functional, as the structures that come from this procedure require fewer optimization steps at the larger basis set. The final optimized structures served as the input to calculate the chemical shifts using the GIAO software included in the PQS software suite. The nuclear magnetic shielding values of the reference molecule, tetramethylsilane (TMS), were also calculated at the B3LYP/6-311++G** level of theory, and the NMR chemical shifts were determined by subtracting the calculated galerucella nuclear magnetic shielding values from the calculated TMS chemical shielding values. The values obtained for the ^{1}H and ^{13}C magnetic shielding of TMS atoms were 31.97 and 184.12 ppm, respectively, at the above level of theory, and the gas-phase ^{13}C experimental value for TMS was ∼186.4.[5]

In addition to the transition-state and energy-minimized structure calculations, ab initio molecular dynamics (AIMD) simulations were performed on the isolated galerucella molecule at the HF/4-31G level of theory, at starting temperatures of 300 and 1000 K. The low-temperature study was performed to account for the single-conformer fluctuations at room temperature, and the high-temperature simulation was performed to observe interconversion between structures on an accelerated time scale. In each simulation, molecular dynamics was performed with constant total energy at a time step of 1.0 fs, starting from the global minimum structure. A total time of 50.0 and 10.0 ps of dynamics was simulated at the high temperature and the lower temperature, respectively. The Verlet method was used to integrate the equations of motion. The dihedral angles that define the conformation of the large ring were output at every time step. For the 300 K simulation, the NMR chemical shifts were calculated for the instantaneous (unoptimized) structure every 20 fs, after an initial 1.0 ps had elapsed. The GIAO calculation of the NMR spectra was done at the B3LYP/6-311++G** level of theory. At the higher temperature, AIMD structures were

(9) *Ab Initio Program Package*, version 3.1; Parallel Quantum Solutions: 2013 Green Acres, Suite A, Fayetteville, AR 72703.
(10) *InsightII/Discover*; Accelrys Software Inc.: 10188 Telesis Court, Suite 100, San Diego, CA 92121.
(11) Cornell, W. D.; Cieplak, P.; Bayly, C. I.; Gould, I. R.; Merz, K., Jr.; Ferguson, D. M.; Spellmeyer, D. C.; Fox, T.; Caldwell, J. W.; Kollman, P. A. *J. Am. Chem. Soc.* **1995**, *117*, 5179−5197.
(12) Baker, J.; Kinghorn, D.; Pulay, P. *J. Chem. Phys.* **1999**, *110*, 4986−4991.
(13) Fukui, K. *J. Phys. Chem.* **1970**, *74*, 4161−4163.
(14) Schmidt, M. W.; Gordon, M. S.; Dupuis, M. *J. Am. Chem. Soc.* **1985**, *107*, 2585−2589.
(15) Anet, F. A. L.; Cheng, A. K.; Krane, J. *J. Am. Chem. Soc.* **1973**, *95*, 7877−7878.
(16) Burkert, U.; Allinger, N. L. *J. Comput. Chem.* **1982**, *3*, 40−46.

TABLE 1. Ring Dihedral Angles (deg), Relative Energies (kcal/mol), and Predicted Populations (at 298 K) of the Unique Conformers with Relative Energies Less than 10.0 kcal/mol

	dihedral angle[a]											
conf.	1−2	2−3	3−4	4−5	5−6	6−7	7−8	8−9	9−10	10−11	Δ*E*	population (%)
A	−67	67	−116	172	−86	−60	166	−63	−48	88	0.00	32.0
B	−68	70	−112	173	−151	55	61	−160	58	40	0.44	15.3
C	42	50	−123	164	−90	−65	165	−93	57	−88	2.20	0.8
D	−40	−55	115	−175	153	−62	96	−156	64	51	2.47	0.5
E	−86	53	47	−175	101	−77	163	−65	−45	81	2.81	0.3
F	42	−60	−39	174	−78	−66	159	−62	−51	70	2.83	0.3
G	−80	71	−109	178	−77	−56	148	−145	55	30	3.04	0.2
H	16	−67	132	−172	102	−80	154	−68	−58	72	3.10	0.2
I	−41	−50	115	−171	94	79	−70	−78	71	54	3.33	0.1
J	65	−73	124	−178	117	−68	138	−151	75	−62	3.41	0.1
K	−59	63	−106	163	−168	57	80	−77	−49	99	3.59	0.1
L	85	−58	100	−176	111	−90	160	−103	50	−81	3.69	0.1
M	105	−43	−52	174	−85	−78	164	−98	51	−76	3.80	0.1
N	−81	59	−94	165	−141	135	−65	−71	72	47	3.89	0.0
O	−51	71	−120	179	−85	−80	76	70	−121	61	3.90	0.0
P	95	−40	−53	175	−163	59	63	−148	75	−58	4.77	
Q	2	56	21	−169	98	−83	158	−95	55	−79	5.03	
R	78	−66	90	173	71	38	56	−154	76	−58	5.36	
S	−90	60	22	180	71	41	58	−159	55	37	5.49	
T	46	−58	−42	177	−140	55	53	−159	60	14	5.89	
U	−101	43	41	−173	76	109	−68	−76	71	45	6.22	
V	−5	−61	−6	178	−77	−53	117	−151	57	40	6.56	
W	−17	−58	126	178	72	26	51	−166	51	42	6.57	
X	−3	−51	−26	171	−113	108	−67	−76	69	46	6.96	
Y	54	−45	−53	164	−156	63	74	−75	−50	66	7.95	
Z	−52	−64	115	−16	−110	178	−63	−69	65	46	9.32	

[a] The dihedral angle numbers refer to the central bond. The preceding and following atom indices are defined to be the adjacent ring atoms; for example, the dihedral angle labeled 1−2 is defined as 14−1−2−3.

periodically optimized to determine what local minimum was most nearly represented by the current structure. The nearest local minimum was determined at least every 500 fs, and more often during conformational changes, to more accurately determine the starting and ending minima associated with the transitions between structures. The 1.0 fs time step employed here is relatively long for the time scale of the bond bending and stretching motions that would be expected here; however, the aim in this study was to explore the conformational space as efficiently as possible, and no explicitly time-dependent quantities were calculated.

Results and Discussion

Table 1 gives the ring dihedral angles, relative energies (at 0 K), and relative populations at 298 K of all of the unique (that is, the Table includes no pairs of mirror images) local minimum-energy structures within 10.0 kcal/mol of the global energy minimum. The ring dihedral angles are referenced by their central bonds, and the outer two atoms that define the dihedral are the adjacent ring atoms; for example, the dihedral angle labeled 1−2 is defined as 14−1−2−3 (see Figure 1). The set of ring dihedral angles uniquely defines each local-minimum conformer. For each of the 26 structures listed in Table 1, there is a mirror-image structure (indicated herein by adding a * to the structure letter) with the identical energy, for which the signs on the dihedral angles are reversed. The relative energies reported in Table 1 are with respect to the energy of conformer A, which has a B3LYP/6-311++G** energy of −484 083.72 kcal/mol.

The two lowest-energy conformers, A and B, are significantly more stable than the others listed in Table 1. These two structures, together with their mirror inverses, account for ~95% of the expected room-temperature distribution of conformers. The structures of the four lowest-energy conformers (A, A*, B, and B*) are shown in Figure 2. Structure B differs from

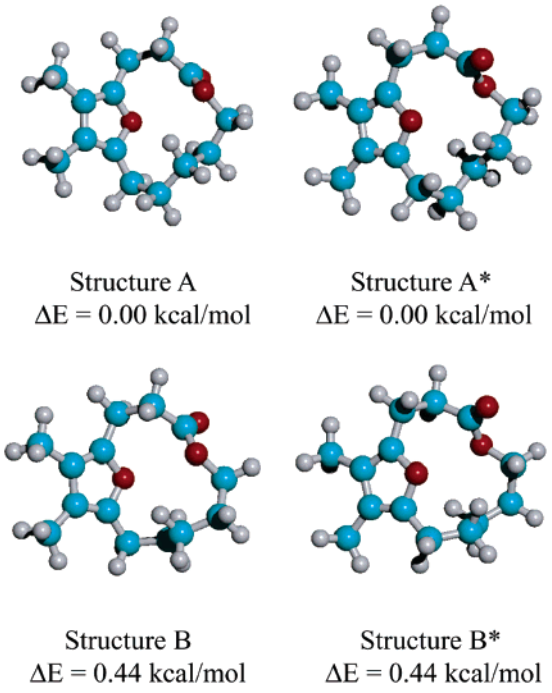

FIGURE 2. Structures A, A*, B, and B* with their relative electronic energies.

structure A by a rotation of the methylene groups at the carbon atoms numbered 7, 8, and 9 in Figure 1. Several pathways were found by which structure A can be converted to structure B; each of these pathways involves a transition through at least one other local minimum (see Figure 7 below). The ester linkage in this molecule can be either cis or trans (the distinction is seen in the value of the 3−4−5−6 dihedral angle); conformer

TABLE 2. Ranges of Ring Bond Lengths (Å) and Bond Angles (deg) for the 26 Conformers Listed in Table 1

bond	range of values	angle	range of values
14−1	1.370 ± 0.005	14−1−2	115.2 ± 1.8
1−2	1.496 ± 0.006	1−2−3	113.6 ± 1.5
2−3	1.546 ± 0.011	2−3−4	114.9 ± 4.3
3−4	1.520 ± 0.006	3−4−5	115.7 ± 5.3
4−5	1.348 ± 0.007	4−5−6	120.4 ± 5.2
5−6	1.451 ±0.005	5−6−7	112.4 ± 4.3
6−7	1.533 ± 0.010	6−7−8	116.0 ± 3.2
7−8	1.543 ± 0.007	7−8−9	116.1 ± 3.1
8−9	1.542 ± 0.006	8−9−10	116.4 ± 3.5
9−10	1.552 ± 0.010	9−10−11	113.6 ± 2.6
10−11	1.496 ± 0.007	10−11−14	114.7 ± 1.7
11−14	1.369 ± 0.006	11−14−1	108.5 ± 0.7

TABLE 3. Ranges of Calculated ^{13}C Chemical Shifts (ppm) Relative to TMS for the 26 Conformers Listed in Table 1

atom	exptl[a]	range of chemical shifts
1	147.00	154.95 ± 1.40
2	22.38	27.30 ± 1.62
3	34.36	36.94 ± 5.73
4	172.00	180.41 ± 2.35
6	62.35	68.76 ± 4.32
7	24.95	33.02 ± 4.76
8	21.86	30.91 ± 6.80
9	24.73	31.56 ± 6.97
10	22.98	28.74 ± 3.16
11	148.00	157.37 ± 2.77
12	115.00	124.42 ± 2.72
13	115.00	124.61 ± 2.29
15	7.50	10.37 ± 0.28
16	7.40	10.52 ± 0.28

[a] The solvent used was perdeuterated benzene, with data taken at 27 °C.

Z, which is 8.32 kcal/mol higher in energy than conformer A, was the most stable conformer found with a cis ester linkage.

Table 2 lists ranges of values for the lactone ring bond lengths and bond angles for the 26 unique conformers listed in Table 1. The first value given for each entry is simply the center of the range. The bond lengths, in general, fall into relatively narrow ranges of values near those one would expect for the types of bonds represented. The 2−3 and 9−10 bonds are somewhat longer than the other carbon−carbon bonds and are the only ones with ranges of values that exceed 0.01 Å. This is likely due to the enhanced 1−4 interactions brought about by the ring strain. The fact that the molecule is cyclic also accounts for the molecule having larger values for the ring bond angles than would be expected in a similar noncyclic system. To examine the effect of the ring on the ester linkage, a B3LYP/6-311++G** geometry optimization calculation was done on the methyl acetate molecule. Compared to methyl acetate, the galerucella C3−C4 and O5−C6 bonds are lengthened by ∼0.01 Å, whereas the C4−O5 bond remains relatively unchanged. The galerucella C−C−O (3−4−5) and C−O−C (4−5−6) bond angles are ∼5° larger than those of methyl acetate.

The experimental ^{13}C NMR chemical shifts, $\delta(^{13}C)$, as well as the ranges of calculated $\delta(^{13}C)$ values for the 26 conformers studied, are reported in Table 3. With few exceptions, the B3LYP/6-311++G** chemical shifts are larger than the experimental values, with the specific values of the chemical shifts generally being conformation dependent. The root-mean-square deviations in the ^{13}C shifts (relative to the experimental chemical shifts) are in the range of ∼6−8 ppm for all of the structures given; this level of root-mean-square (rms) deviation from experiment is to be expected from B3LYP calculations.[5] The calculated chemical shifts for the methyl carbons are noticeably more homogeneous than those of the carbon atoms that make up the large ring. The methyl groups are so remote from the flexible ring that the local magnetic environment does not change significantly with ring conformation and the calculated methyl $\delta(^{13}C)$ values remain about 3 ppm higher than the experimental values for all of the conformers studied. Because these values are relatively independent of the conformation, it is clear that there is a systematic error in the calculated ^{13}C peaks, resulting from either the calculation method or solvent interactions. The next smallest range of $\delta(^{13}C)$ is found on carbon atom 1; the relatively short hydrocarbon chain between that atom and the ester group, together with the fact that the atom is a part of the inflexible furan ring, results in a narrow range of possible through-space interactions between the oxygen atoms and that carbon atom. On the other hand, the flexibility of the large ring accounts for relatively broad ranges of magnetic environments at carbons 3, 8, and 9, as there are many possible distances between these atoms and the three oxygen atoms, depending on the ring conformation.

TABLE 4. Ranges of Calculated ^{1}H Chemical Shifts (ppm) Relative to TMS for the 26 Conformers Listed in Table 1[a]

carbon atom	exptl	range of values
2	2.80	2.96 ± 0.11
3	2.27	2.53 ± 0.31
6	4.20	4.27 ± 0.34
7	1.63	1.35 ± 0.63
8	1.24	1.51 ± 0.83
9	1.50	1.78 ± 0.38
10	2.54	2.58 ± 0.16
15	1.78	1.90 ± 0.04
16	1.70	1.92 ± 0.05

[a] The calculated ranges reflect an averaging over hydrogen atoms attached to each carbon atom.

Table 4 lists the experimental and ranges of calculated $\delta(^{1}H)$ values for the 26 conformers listed in Table 1. The atom numbers are those of the carbon atoms to which the hydrogen atoms are attached. Because the experimental ^{1}H NMR spectrum shows only a single signal for each set of methylene (or methyl) protons on a given carbon atom, the chemical shift values in Table 4 reflect averages of the calculated signals for the protons on each carbon atom. In Table 4, the smallest variation in average $\delta(^{1}H)$ is on the methyl groups attached to the furan ring, which are consistently ∼0.1−0.3 ppm higher than the experimental values. The methylene hydrogen atoms attached to carbon 2 exhibit the next smallest range, again owing to the relatively small range of local environments available to that portion of the molecule among the various conformers. The solvent used in the experimental study was perdeuterated benzene; this solvent has been shown to change chemical shifts when compared to deuterated chloroform (historically, a "standard" NMR solvent) by up to 1 ppm or more.[17] Accordingly, solvation effects could be the cause of some of the deviations between the experimental and calculated chemical shifts.

Because there is clearly a systematic difference present between the calculated and experimental chemical shifts, a least-squares linear regression analysis was performed on each NMR data set (^{1}H and ^{13}C) for each of the conformers. In this analysis, the calculated chemical shifts were taken to be a function of the experimental shifts, and the least-squares line was deter-

(17) Laszlo, P. *Prog. Nucl. Magn. Reson. Spectrosc.* **1967**, *3*, 231−402.

TABLE 5. Standard Deviations in the *y* Axis Obtained from Least-Squares Linear Regression Analysis on the Calculated Chemical Shifts

conf.	ΔE	std deviation in *y* values ^{13}C	^{1}H
A	0.00	1.45	0.067
B	0.44	1.98	0.108
C	2.20	2.65	0.442
D	2.47	2.18	0.283
E	2.81	1.94	0.123
F	2.83	1.80	0.100
G	3.04	2.15	0.155
H	3.10	2.14	0.137
I	3.33	3.45	0.404
J	3.41	3.16	0.256
K	3.59	2.65	0.068
L	3.69	2.67	0.275
M	3.80	2.35	0.392
N	3.89	2.65	0.191
O	3.90	3.19	0.146
P	4.77	1.74	0.342
Q	5.03	3.04	0.363
R	5.36	1.31	0.281
S	5.49	2.01	0.252
T	5.89	2.31	0.101
U	6.22	3.11	0.328
V	6.56	2.94	0.260
W	6.57	2.05	0.324
X	6.96	3.28	0.313
Y	7.95	2.54	0.148
Z	9.32	3.68	0.343

mined. By looking at the standard deviations in the *y* values about the line (i.e., the residual for each data set, σ_y), we effectively subtracted out the systematic error predicted for that set of data. The calculated shifts corresponding to the best structure should be characterized by low σ_y values for both the ^{1}H and ^{13}C spectra. Table 5 lists the σ_y values for the ^{1}H and ^{13}C calculated chemical shifts for each of the minimum-energy galerucella conformers listed in Table 1. Prior to performing the $\delta(^{1}H)$ regressions, the signals from equivalent hydrogen atoms were averaged. Figure 3 gives scatter plots with the σ_y values for each conformer plotted against the energies. Each diamond represents a conformer, and selected conformers are labeled in the scatter plot. In considering both the calculated energy and calculated NMR shifts, we would expect that the best conformers would be represented by data points toward the lower left of each scatter plot.

The smallest deviation in the ^{13}C spectrum is seen for conformer R, which is 5.36 kcal/mol less stable than structure A, suggesting that comparison to the experimental CMR spectrum alone is not a completely satisfactory means of confirming the identity of the most stable conformer. This fact is confirmed in that structure R's $\delta(^{1}H)$ values do not match the experimental spectrum particularly well. Conformer A has the second closest set of ^{13}C shifts to the regression line, and structure B has the sixth smallest regression residual for the CMR spectrum. For the ^{1}H data, conformer A gives the lowest residual at 0.067 ppm, and conformer B is again considerably better than average, at 0.108 ppm. Conformer K ($\Delta E = 3.89$) shows a small σ_y value for the ^{1}H chemical shifts, but the ^{13}C chemical shifts do not match the experiment very well. Conformers A and B stand out in Figure 3 as both being significantly lower in energy than the other conformers and having relatively small deviations from the calculated best-fit lines of calculated vs experimental chemical shifts.

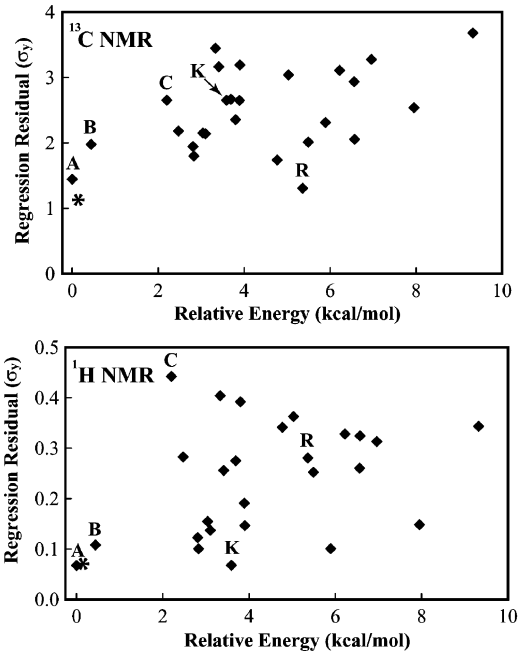

FIGURE 3. Scatter plots of NMR chemical residuals vs relative energies. Top frame: regression residuals from ^{13}C chemical shifts. Bottom frame: regressions from ^{1}H chemical shifts.

TABLE 6. Experimental and Calculated ^{13}C NMR Chemical Shifts (ppm) for the Four Lowest-Energy Conformers

atom	exptl	conformer A	A*	B	B*	av	(calcd − exptl)
1	**146.10**	155.61	155.61	156.13	156.14	**155.78**	**9.77**
2	**22.38**	28.13	28.12	28.32	28.33	**28.19**	**5.84**
3	**34.36**	40.28	40.26	40.60	40.61	**40.38**	**6.08**
4	**172.00**	180.40	180.40	181.14	181.14	**180.64**	**8.77**
6	**62.35**	68.07	68.07	64.63	64.64	**66.96**	**4.00**
7	**24.95**	29.49	29.47	31.41	31.41	**30.10**	**5.49**
8	**21.86**	27.58	27.58	25.32	25.32	**26.85**	**4.59**
9	**24.73**	33.31	33.32	26.05	26.05	**30.96**	**4.95**
10	**22.98**	26.98	26.97	29.04	29.03	**27.64**	**5.02**
11	**147.60**	157.56	157.54	156.26	156.26	**157.13**	**9.31**
12	**114.40**	123.70	123.69	125.10	125.11	**124.15**	**10.00**
13	**114.40**	124.00	123.99	123.61	123.61	**123.87**	**9.40**
15	**7.40**	10.58	10.57	10.53	10.53	**10.56**	**3.15**
16	**7.50**	10.74	10.74	10.72	10.71	**10.73**	**3.23**
std dev in *y* values		1.45	1.45	1.98	1.98	**1.13**	

The calculated ^{13}C and ^{1}H NMR chemical shifts for the four lowest-energy structures are given in Tables 6 and 7, respectively, along with the experimentally observed chemical shifts. For each conformer, the calculated chemical shifts are averaged for the methyl hydrogen atoms. Tables 6 and 7 also give the Boltzmann-weighted average (at 298 K) of the calculated chemical shifts, which would be the expected signal if interconversion among the four minima occurred rapidly on the NMR time scale. The deviations of these average shifts from the experimentally observed shifts occupy the last column in Tables 6 and 7. The theory vs experiment linear regression analysis was performed, and the standard deviations in *y* values for the averaged conformer are reported at the bottom of Tables 6 and 7. This averaged conformer is represented by the asterisks in Figure 3. Taking the Boltzmann-weighted average of the ^{13}C chemical shifts of conformers A and B results in a significant improvement in the theory vs experiment plot, with a lower residual for the averaged conformer than that seen for any of

TABLE 7. Experimental and Calculated ^{1}H NMR Chemical Shifts (ppm) for the Four Lowest-Energy Conformers

		conformer					(calcd −
atom	exptl	A	A*	B	B*	av	exptl)
2a	**2.78**	3.18	2.62	3.13	2.67	**2.90**	**0.12**
2b	**2.78**	2.62	3.18	2.67	3.13	**2.90**	**0.12**
3a	**2.26**	2.21	2.35	2.12	2.37	**2.27**	**0.01**
3b	**2.26**	2.35	2.21	2.37	2.12	**2.27**	**0.01**
6a	**4.20**	3.38	5.14	3.63	4.99	**4.28**	**0.08**
6b	**4.20**	5.14	3.38	4.99	3.63	**4.28**	**0.08**
7a	**1.62**	1.06	2.55	1.96	1.37	**1.76**	**0.14**
7b	**1.62**	2.54	1.06	1.38	1.96	**1.76**	**0.14**
8a	**1.24**	1.33	1.25	1.19	1.14	**1.25**	**0.01**
8b	**1.24**	1.25	1.33	1.14	1.19	**1.25**	**0.01**
9a	**1.50**	1.53	1.65	2.15	1.34	**1.64**	**0.14**
9b	**1.50**	1.65	1.53	1.34	2.15	**1.64**	**0.14**
10a	**2.53**	2.61	2.74	2.47	2.70	**2.64**	**0.11**
10b	**2.53**	2.74	2.61	2.70	2.47	**2.64**	**0.11**
15a−c	**1.77**	1.92	1.92	1.89	1.89	**1.91**	**0.14**
16a−c	**1.70**	1.92	1.92	1.91	1.91	**1.92**	**0.22**
std dev in *y* values		0.067	0.067	0.108	0.108	**0.071**	

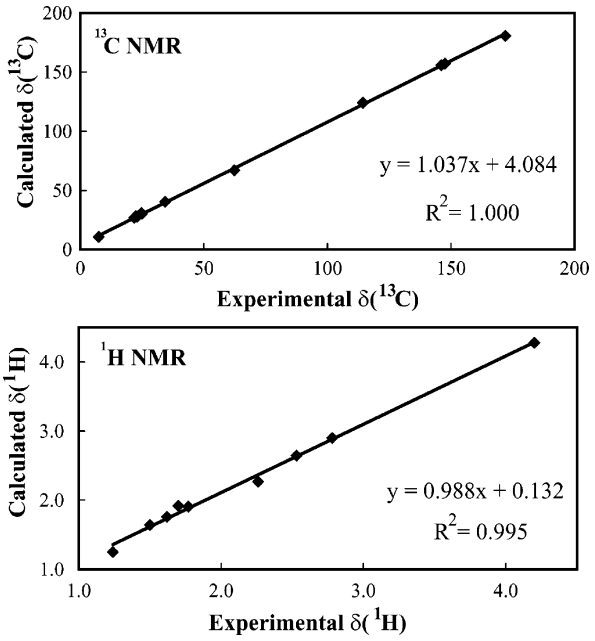

FIGURE 4. Least-squares fit of the calculated vs experimental relative ^{13}C and ^{1}H chemical shifts. Units on both axes are parts per million.

the individual conformers. In the case of the ^{1}H data, the averaged conformer has a residual only slightly higher than that associated with conformer A. In examining the individual ^{1}H deviations from the experimental data, it is apparent that all of the chemical shifts for both conformer A and conformer B are within 0.30 ppm of the experimental values; there are only two other conformers (E and K) for which this is the case. In the averaged spectrum, the only $\delta(^1H)$ peak that deviates by more than 0.2 ppm from the experimental result arises from one of the two methyl groups. As mentioned earlier, the deviations in the methyl group chemical shifts are largely independent of the specific conformer.

Figure 4 displays plots of the calculated vs experimental ^{13}C and ^{1}H chemical shifts, where the calculated values are the averaged values of Tables 6 and 7. The equations of the best-fit lines and the r^2 (1.000 and 0.995, respectively) values associated with those linear least-squares fits are given in the

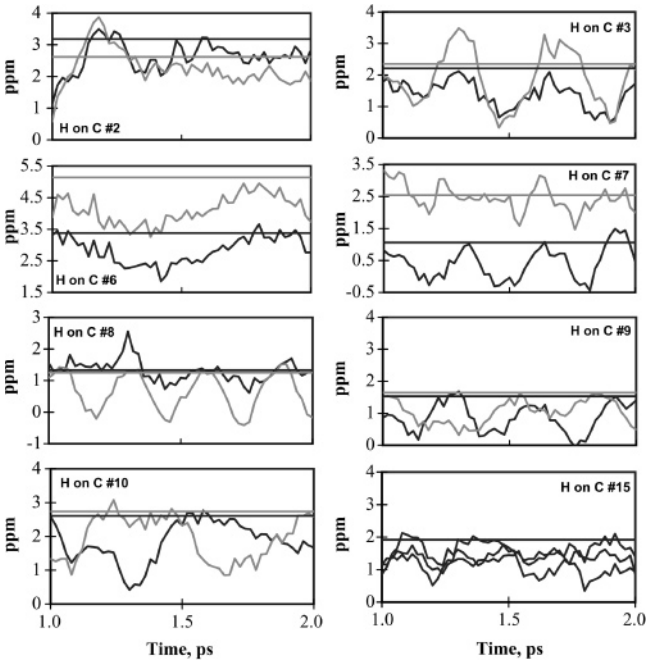

FIGURE 5. Time-dependent calculated relative chemical shifts from conformers found during the 300 K ab initio molecular dynamics simulation, starting from conformation A in the schematic diagram on the right.

insets. Both sets of data are highly linear, with slopes (1.033 and 0.987, respectively) close to unity. The calculated spectra thus match the experimental ones very well, when allowance is made for the systematic shift characteristic of GIAO calculations at the level of theory employed here.[5]

In looking at an individual 0 K structure, the anisotropic nature of the hydrogen chemical shifts is apparent (see Table 7), particularly when the hydrogen atoms in question are connected to a carbon atom that interacts strongly with a nearby oxygen atom (e.g., the hydrogen atoms on carbon 6). That each set of methylene hydrogen atoms gives rise to only a single signal indicates that structural interconversion and/or vibrational fluctuations tend to average out the magnetic environments surrounding the two "equivalent" atoms. Figure 5 displays the time-dependent ^{1}H chemical shifts that were calculated during the 300 K AIMD simulation in structure A. No transitions to other conformers were observed during this simulation, so the oscillations in the chemical shifts are due to the predicted room-temperature vibrations that would occur over a very short period of time. In each frame, the predicted 0 K chemical shifts of the two equivalent methylene hydrogen atoms are plotted with horizontal lines. In the lower right frame, the shifts for the three methyl hydrogen atoms on one of the methyl groups are plotted together, along with the averaged 0 K shift. The ring dihedral angles were plotted as a function of time (not shown for this simulation), and Figure 5 represents a sufficiently large set of data points to include at least one full oscillation of each of the dihedral angles, on the longest time scale observed. From Figure 5, it is clear that some of the pairs of methylene hydrogen atoms tend to move toward a similar average environment at 300 K, whereas others remain completely separated throughout the simulation. The hydrogen atoms on carbons 6 and 7, owing to their proximity to the ester group, do not see similar magnetic environments, even when molecular motion is taken into account. Accordingly, it is clear that some interconversion

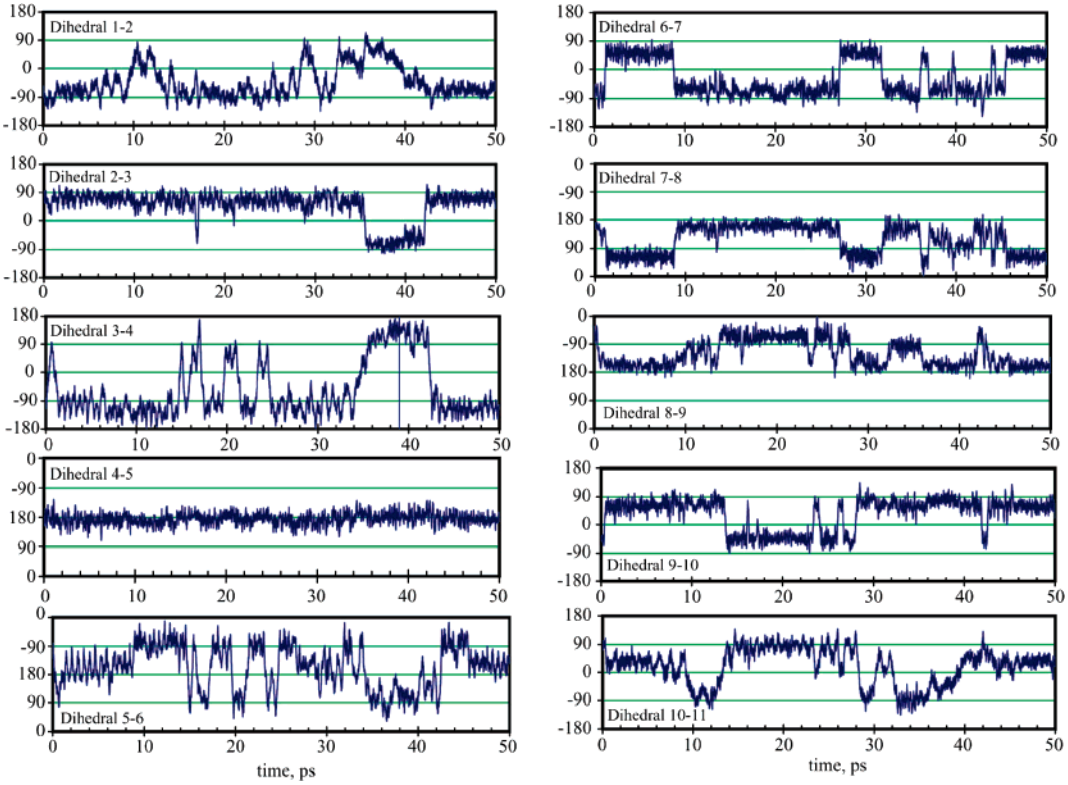

FIGURE 6. Variation of the ring dihedral angles (deg) during the 1000 K ab initio molecular dynamics simulation. Note that the dihedral angle scales in several frames are shifted.

between structures must occur for all the pairs of methylene hydrogen atoms to appear equivalent in the experimental NMR spectrum.

To allow for the interconversion between structures on a time scale which can practically be simulated using ab initio molecular dynamics, it was necessary to model the dynamics at an artificially high temperature. In Figure 6, the ring dihedral angles are shown as a function of time during the 50 ps ab initio molecular dynamics run which was performed, starting from conformer A, at a starting temperature of 1000 K. The 4−5 dihedral angle is the only one that undergoes no significant change during the simulation, oscillating around 180° throughout the run. Several structural transitions are evident from the abrupt changes in the dihedrals. It is evident that some of the bonds are more flexible than others; for example, although the 5−6 dihedral oscillates between the values characteristic of A and A*, it is relatively infrequently that the 2−3 dihedral changes from its oscillation about 60°. Considering this molecular dynamics simulation, there are two points to be stressed. First, the simulation was performed at the HF/4-31G level of theory, which gives energies that differ from the B3LYP/6-311++G** energies for the local minima and transition states. The general trend is for the HF/4-31G calculations to give transition states that are ∼1−2 kcal/mol higher in energy (relative to structure A) than the B3LYP/6-311++G** calculations. Second, the molecular dynamics (MD) calculation was performed on an isolated molecule under constant energy conditions. In the real system, energy transfer between the galerucella molecule and its solvent environment may occur fast enough to allow for thermal equilibrium (for which a constant temperature simulation would be appropriate, rather than one performed at constant molecular energy). Finally, the 50 ps duration of the MD simulation is a very short period of time, relative to the time scale of the NMR experiments.

Figure 7 plots the HF/4-31G energies of the optimized structures for those points during the simulation at which energy-minimized structures were obtained. The points are not evenly spaced, as optimizations were more frequently performed in regions of the simulation where structural transitions were taking place, as evidenced by large changes in one or more of the ring dihedrals (cf. Figure 6). The inset shows a "map" of connected conformers that summarizes the transitions observed during the simulation. Figure 7 shows that there is relatively free interconversion among a subset of structures at this artificially high temperature. Full inversion from A to A* was not observed during the course of the simulation, nor was any other conformer found to convert into its inverse structure in the time period studied; however, 12 of the calculated minimum-energy conformers were visited during the simulation. The residence time in structure B is longer than that of any other state (including state A); this is because the transition-state energies for the transitions out of state B are somewhat higher than the transition-state energies for transitions out of state A (see Figure 8, below). State G′, observed twice in the simulation, is an artifact of the small basis set employed; upon optimization at B3LYP/6-311++G**, conformer G′ converted to conformer G. In all, 255 minimizations were performed at the HF/4-31G level of theory to find the closest minima to the AIMD structures. Of these, only two failed to converge, and a few more converged to structures that were obviously meta-stable conformers that were similar to previously identified minima.

To determine if the full inversion from structure A to its mirror image is a likely possibility at room temperature, the transition states between the various local minima were studied,

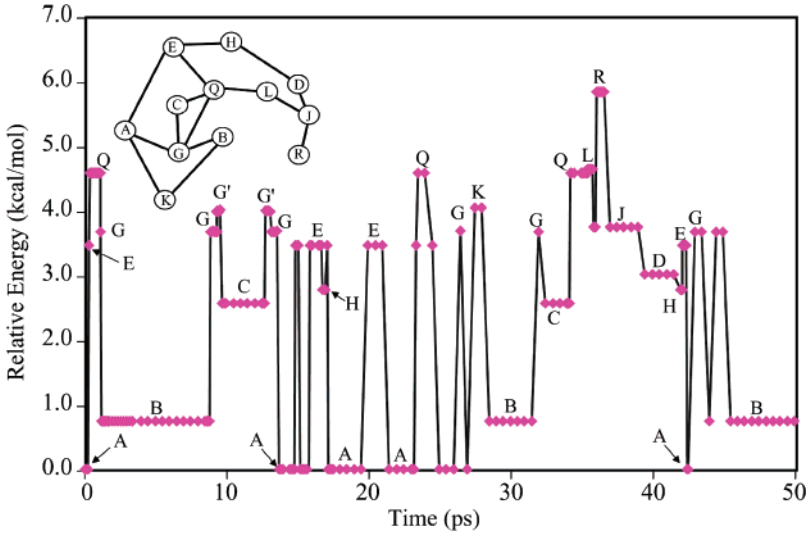

FIGURE 7. Conformers visited during the 50 ps ab initio molecular dynamics simulation plotted against the relative energy of each upon energy minimization at the 4-31G basis set. Inset: A "map" that displays the transitions between conformers observed during the simulation.

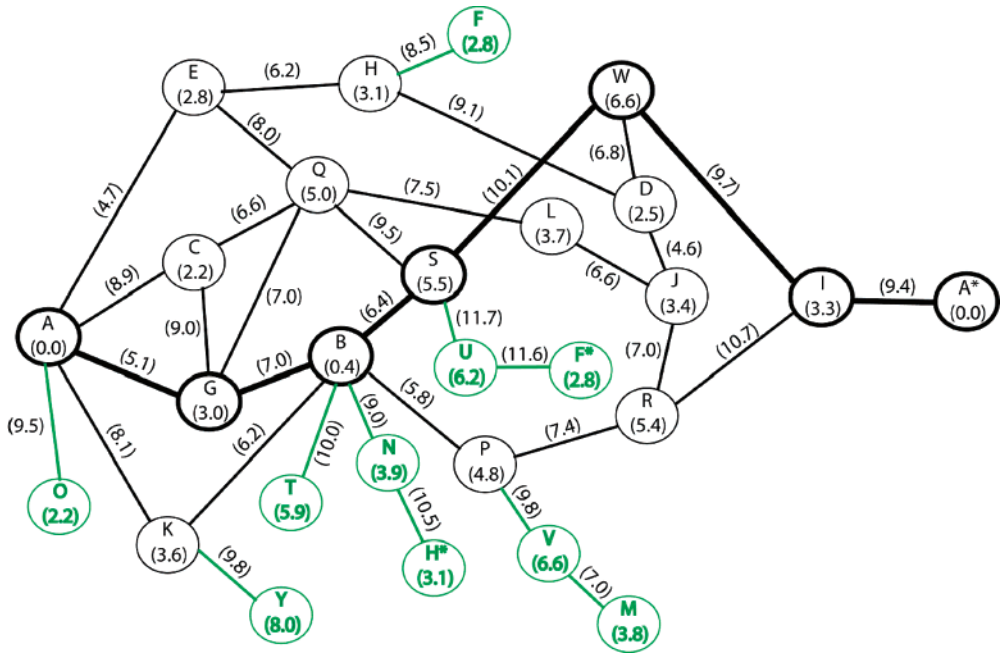

FIGURE 8. "Map" of energy-minimized conformers with their relative energies (DFT) in the circle and transition state barriers in parentheses along the path between conformer states. The heavy line follows one possible path from conformer A to its inverse A*.

and a pathway between structures A and A* was generated. The conformer map, containing the connections between observed local minima, is shown in Figure 8. Inside the ovals, along with the conformer labels, are the relative (B3LYP/6-311++G**) energies of the local minima; the transition-state relative energies are given in parentheses along the lines connecting the minima. Through a series of transition states, several potential pathways can be followed from structure A to structure A*, many of which involve structure B as an intermediate. Local minima (and transitions to those minima) which are not part of an A → A* pathway are indicated in gray. It should be noted that an "inverse" map, with all of the structures exchanged with their mirror images, also exists; this could contain the most favorable pathway for conversion from A* back to A, with the conformer B* as an intermediate. One relatively favorable pathway for the A → A* inversion is indicated with heavier lines. Because of the number of possible conformers and the number of degrees of freedom available for the ring conformation process, it is possible that there are transition states and minima other than those reported here. However, Figure 8 illustrates that there are several possible pathways for conversion of conformer A to its mirror-image structure and that facile interconversion between conformers A and B (and thus also between A* and B*) is almost certainly possible at room temperature.

The connection between conformers G and Q illustrates an interesting problem that arises in the calculation of transition states. In the molecular dynamics run, this transition was narrowed down to a 2 fs range, and HF/4-31G mode-following calculations produced the same transition state, on both sides

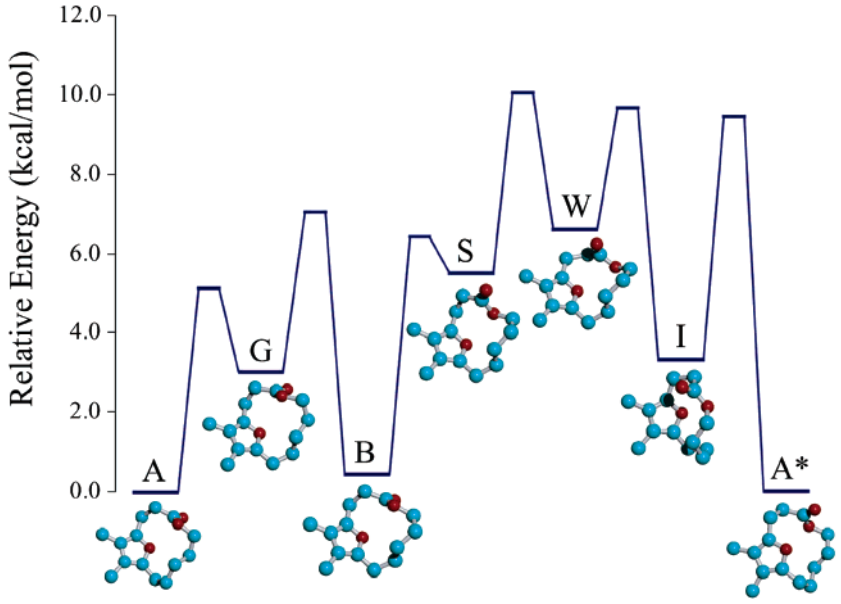

FIGURE 9. Relative energies of the minima and transition states along the conformer interconversion path denoted by the heavy line in Figure 8.

of the transition, following each of the first five modes on both sides. However, this same transition state was just as decisively found to link states G and B, using a mode-following calculation from the minimum-energy conformation G (also at the HF/4-31G level of theory). Furthermore, a reaction path following calculation at the B3LYP/6-311++G** level from the transition state produced state B, rather than state Q. There were two other instances in which the transition states obtained seemed to link two pairs of states (in each case, there were a total of three different minimum-energy conformers involved). Because the geometry obtained, in each case, was consistent with both reaction paths, it was assumed that the transition state was valid for both transitions. The complexity of the conformation space for this molecule is such that it is expected that there may be more than two downhill paths from a given transition state.

Figures 9 and 10 illustrate the structures observed along the interconversion pathway that is shown in bold lines in Figure 8. In Figure 9, the B3LYP/6-311++G** energies of the minima and transition states are plotted, and the structures of the various local minima are shown below the corresponding energies (with the hydrogen atoms removed from the displayed structures). Figure 10 plots the values of the dihedral angles along the inversion path, with points plotted for both the minima and the transition states. In the highlighted pathway, the first transition, from A → G, involves a rearrangement of the methylene groups in the longer chain (shown at the bottom of the molecule), with significant changes in the 8−9, 9−10, and 10−11 dihedrals. The molecule then converts into structure B by rearrangements of the other three dihedrals in the long methylene chain. Structure B is surrounded by barriers of ∼6−10 kcal/mol (cf. Figure 8), so it would be expected to be fairly kinetically (as well as thermodynamically) stable, as was observed in the discussion of the higher-temperature MD simulation. The next step in the sequence is the flip of the ester group (from B → S), involving changes in the 3−4 and 5−6 dihedral angles. Following the ester flip, the molecule converts from conformer S to conformer W by a rearrangement of the shorter methylene chain (shown at the top of the molecule). This is followed by another rearrangement in the long methylene chain, to get to conformer I. In the final step, the furan ring rotates (as seen by changes in the 1−2 and 10−11 dihedral angles), accompanied by changes in the 7−8 and 8−9 dihedral angles, resulting in the full inversion to conformer A*. Throughout this process, most of the dihedral angles change in an approximately unidirectional fashion, with the exception of dihedral 8−9, which changes from approximately −60° to −160°, then back through 0° to +60°. The dihedral angle defined around the 4−5 bond is relatively unchanged during the inversion sequence; it remains at ∼180° in the transition states and the local minima. Figure 10 also shows that, although two or three dihedral angles may be coupled for an individual transition, those couplings between dihedrals are not perfectly general and can change from step to step. Accordingly, it is not straightforward to define a single reaction coordinate (or reduce the problem to two or three coordinates) for the inversion process. The problem of defining a simple reaction coordinate is further complicated by the fact that the direction of change of a given dihedral angle (i.e., whether through 0° or 180°) is not always obvious.

Looking back at the transitions observed in the 1000 K molecular dynamics run (Figure 7), the dynamics confirms the connections from state A to states E, G, and K (the three transitions with the lowest-transition-state energy barrier). When the simulation found the molecule in state B, the only pathway to a different conformer was to step G. This is likely due to differences in the predicted transition states between the two computational methods. Conformer R was visited at one point in the simulation; in principle, this structure is only two conformational changes removed from structure A*. It is likely, then, that a significantly longer AIMD simulation at this elevated total energy would have produced a full inversion from A to A*, although not necessarily along the pathway highlighted in Figures 9 and 10.

Conclusions

Through an extensive series of density functional calculations, 52 different structures for the galerucella pheromone have been

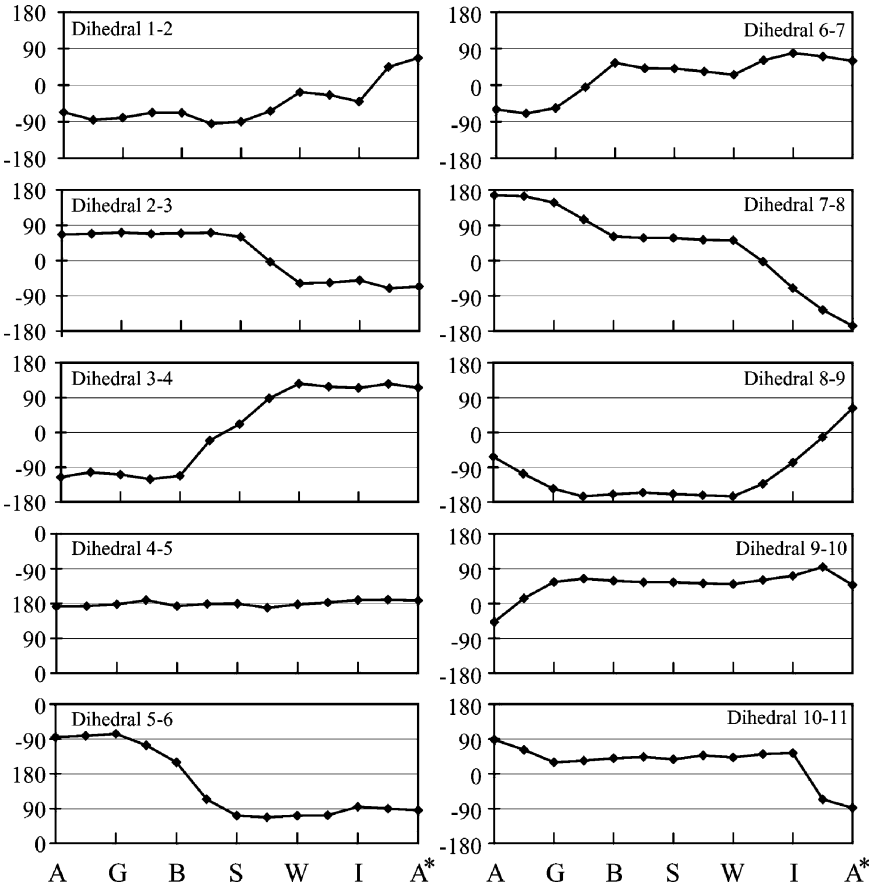

FIGURE 10. Changes in large ring dihedral angles (deg) as the molecule proceeds between energy-minimized conformations in the transition between conformers A and A* along the path described in Figure 9.

identified that are within 10.0 kcal/mol of the lowest-energy structure. Furthermore, the transition states between many pairs of these states have been found so that pathways to full interconversion between the two lowest-energy structures (A and A*) could be identified. Many of the transitions between the various conformers were verified using an ab initio molecular dynamics simulation at high temperature. In comparing the different conformers, we found that the calculated ^{1}H and ^{13}C NMR spectra for the lowest-energy conformers are among the best after systematic deviations are removed, and the Boltzmann-averaged ^{13}C NMR shifts match the experimental data better than the shifts calculated for any of the individual conformers. This offers further evidence, beyond the relative energies, that the experimentally observed conformers of this molecule have been found.

It is likely the case that the galerucella molecule, in the solution phase, consists of a mixture of conformers A, A*, B, and B*. If fast interconversion between these structures can take place in solution, the best theoretical predictions for the NMR chemical shifts come from averaging the chemical shifts calculated for these four lowest-energy structures (cf. Tables 6 and 7). These averaged ^{1}H and ^{13}C NMR results agree well with the experimental spectra. Some of the pairs of methylene hydrogen atoms may experience a similar magnetic environment, leading to a single signal for two hydrogen atoms, simply as a result of the molecular vibrations of a single conformer as shown in the room-temperature dynamics simulation. For some of the methylene groups, this is not the case, however, so some change in conformation must be taking place that effectively exchanges the environments of the two hydrogen atoms, suggesting ring inversion is taking place. Experimental Gibbs free energies of inversion may be obtained by measuring the temperature above which coalescence of the ^{1}H NMR peaks occurs.[15] The reverse prediction, i.e., whether the peaks would be expected to have coalesced at a given temperature given the transition-state energies, is less straightforward for a multistep path inversion, such as the ones described here. For transitions from conformers of higher energy, the height of the effective barrier depends on whether the molecule can come to thermal equilibrium with the solvent on a time scale that is short compared to the residence time in that state.

Acknowledgment. Names are necessary to report factually on available data; however, the USDA neither guarantees nor warrants the standard of the product, and the use of the names by the USDA implies no approval of the product to the exclusion of others that may also be suitable. W.B. acknowledges the Biotechnology Research and Development Corporation (BRDC) for grant support during a sabbatical leave.

Supporting Information Available: Coordinates and energies of the 26 energy-minimized structures. This material is available free of charge via the Internet at http://pubs.acs.org.

JO0524730